Investigating the microenvironmental effects of scaffold chemistry and topology in human mesenchymal stromal cell/polymeric hollow microfiber constructs

Claudio Ricci,[1] Luisa Trombi,[1] Ilaria Soriga,[2] Fabio Piredda,[2] Mario Milazzo,[3] Cesare Stefanini,[3,4] Luca Bruschini,[1,5] Giuseppe Perale,[6] Gianni Pertici,[6] Serena Danti[1,3,7]

[1]OtoLab, Azienda Ospedaliero-Universitaria Pisana, Pisa; [2]Department of Chemistry, Materials and Chemical Engineering, Politecnico di Milano, Milan; [3]Creative Engineering Design Area, Biorobotics Institute, Scuola Superiore Sant'Anna, Pontedera (PI), Italy; [4]Department of Biomedical Engineering, Khalifa University, Abu Dhabi, UAE; [5]Department of Surgical, Medical, Molecular Pathology and Emergency Medicine, University of Pisa, Pisa, Italy; [6]Department of Innovative Technologies, University of Applied Sciences and Arts of Southern Switzerland, Manno, Switzerland; [7]Department of Civil and Industrial Engineering, University of Pisa, Pisa, Italy

Abstract

Tissue engineering scaffolds have shown an intrinsic ability to provide cellular stimulation, thus behaving as physically active microenvironments. This study reports on the interaction between human mesenchymal stromal cells (hMSCs) and dry-wet spun polymer microfiber meshes. The following scaffolding parameters were tested: i) polymer type: poly-L-lactide (PLLA) *vs* poly-ε-caprolactone (PCL); ii) non-solvent type: ethanol (Et-OH) *vs* iso-propanol/gelatin; iii) scaffold layout: patterned *vs* random microfiber fabrics. After two culture weeks, the effects on metabolic activity, scaffold colonization and function of undifferentiated hMSCs were assayed. In our study, the polymer type affected the hMSC metabolic activity timeline, and the metabolic picks occurred earlier in PLLA (day 6) than in PCL (day 9) scaffolds. Instead, PLLA *vs* PCL had no endpoint effect on alkaline phosphatase (ALP) activity expression. On average, the hMSCs grown on all the random microfiber fabrics showed an ALP activity statistically superior to that detected on patterned microfiber fabrics, with the highest in Et-OH random subtypes.

Such findings are suggestive of enhanced osteogenic potential. The understanding of scaffold-driven stimulation could enable environmental hMSC commitment, paving the way for new regenerative strategies.

Introduction

About two decades ago, tissue engineering was proposed as an emerging trans-disciplinary field to generate three-dimensional (3D) tissue substitutes *ex vivo* aimed at accomplishing unmet clinical needs and enabling new regenerative therapies.[1] Nowadays, viable 3D cellular constructs have been successfully obtained in the laboratory by culturing cells under extrinsic stimulation factors on 3D biomaterial-based scaffolds. These are used to act as temporary templates for 3D organization and differentiation of stem cells (SCs), leading to translational approaches.[2,3] Among the adult SCs, the mesenchymal stem (or stromal) cells (MSCs) provide a very useful and accessible cell source and are employed as an effective tool to obtain several differentiated cellular types, in particular those deriving from mesodermal tissues, such as osteoblasts, chondroblasts, myoblasts and adipoblasts.[4] Indeed, musculoskeletal tissues are often affected by pathologies for which surgical tissue replacements are broadly needed, thus making MSC-based therapies highly appealing.[5] The use of undifferentiated cells has posed the challenge of finely tuning and controlling their differentiative profiles; this is usually obtained *in vitro* by providing the constructs with chemical (*e.g.*, soluble factors) or, more recently, mechanical (*e.g.*, stresses via fluid dynamics) stimuli through the culture media (CM).[6] Nonetheless, one of the most recent frontiers in controlling SC behavior is represented by the application of specific physical stimuli, inherently induced by the scaffold as a microenvironment.[7] Indeed, interfacing SCs with defined biomaterial cues (*e.g.* certain types of surface topology and material stiffness) has been reported to affect their biology, thus accrediting the scaffold not only as a merely passive substrate for cellular organization, but rather as an active component of tissue-engineered systems.[8]

A number of scaffolding technologies have been developed over the last two decades with the primary intent of efficiently housing the cells within proper 3D settings.[9] Fiber-based scaffolds offer highly customizable features, ranging from nano- to micro-scale, owing to the many possibilities offered for tailoring fibers and fabrics.[10] Among them, meshes of ultrafine (<10 μm) fibers produced via electrospinning are probably the best investigated in tissue engineering.[11] However, the architectural features and thickness limitations of electrospun scaffolds have restricted their applications to replace the bi-dimensional defects of soft connective tissues.[12,13] Instead, large diameter (>100 μm) microfiber scaffolds, produced via 3D printing or other spinning apparatuses, do not show any limitations of thickness, making them true 3D scaffolds. The hollow microfibers, also referred to as microtubules, belong to the large-diameter microfiber class and can be manufactured via dry-wet spinning.[14] This technique exploits ternary (or multi-) component miscibility to produce fibers from solutions. Basically, in order to be spun, the (co)polymer is dissolved inside a solvent (or solvent mixture), while a non-solvent (or solvent mixture) is concomitantly used to

obtain the fiber cavity. Upon drying, the wet fiber solidifies under a ternary (or multi-) component system, whose miscibility gaps ultimately tailor the fiber morphology. Although very appealing in terms of manufacturing, the necessity for solvents and non-solvents poses potential cytotoxicity issues for biomedical use. So far, regenerative opportunities offered by hollow microfiber scaffolds have been the subject only of a limited number of studies.[14-19] A decade ago, Lazzeri *et al.* reported on the fabrication of bioresorbable dry-wet spunmicrofibers emphasizing their versatility of incorporating nanoparticle-loaded drugs useful for tissue engineering applications.[14] Later on, Ellis *et al.* produced microfiber membranes by phase inversion and tested them using an immortalized osteoblast cell line. These authors envisioned that hollow microfiber scaffolds could be interesting bone substitutes for centimeter-size defects, with fiber cavities possibly accommodating capillary and small vasculature infiltration.[15] Other *in vitro* studies, mostly performed by the authors of this research, have shown that hollow microfiber bonded scaffolds were capable of supporting osteoblast, fibroblast and myoblast cell lines, as well as primary chondrocytes, umbilical cord and bone marrow MSCs, thus appearing widely suitable for musculoskeletal tissue regeneration.[16-19] However, no lineage specification driven by dry-wet spun scaffolds has been assessed so far. Recently, some reports have suggested that other fibrous scaffolds can play biomimetic roles on cellular organization.[20,21] The microenvironmental effects intrinsically induced by the scaffolds become particularly important when undifferentiated cells, like the SCs, are used, since topological stimuli can affect, on multi-scale orders, cell attachment, growth up to differentiation.[7,8] Owing to its strategic relevance, the understanding of scaffold-induced cellular stimulation deserves additional and systematic investigative efforts in regenerative therapies.

This study was aimed at fabricating 3D dry-wet spun microfiber scaffolds for tissue engineering applications. Therefore, the influence played by polymer, non-solvent and fabric layout upon human MSC (hMSC) culture, was studied. The poly-L-lactic acid (PLLA) and the poly-ε-caprolactone (PCL), both approved for clinical practice, were tested as polymers, while ethanol (Et-OH) and isopropanol/gelatin (IP-OH/G) water solutions were used as non-solvents. The obtained hollow microfibers were assembled either orderly or randomly, so as to provide different topologic cues for cellular organization. The investigation of biological effects on hMSC behavior possibly caused by the abovementioned parameters was carried out by assaying metabolic activity, viability, 3D organization and expression of alkaline phosphatase (ALP) activity, the latter as a con-stitutive marker of these cells that is additionally imputed in their proneness to osteogenic differentiation.

Insight into fabrication parameters affecting hMSC behavior on microtubule meshes could enable new knowledge and ultimately define novel routes to control hMSC fate via architectural and chemical parameters.

Materials and methods

Materials

For scaffold manufacturing, the following materials were purchased and used without modifications: PLLA, $M_w \approx 200,000$ and iv=1.4 (Purac Biochem, Gorkum, Netherlands); PCL, $M_n \approx 80,000$ (Sigma-Aldrich, St. Louis, MO, USA); dichloromethane (Sigma-Aldrich); Et-OH, 95% vol. and IP-OH, 50% vol. [Carlo Erba Reagenti, Cornaredo (MI) Italy]; gelatin (G), CAS Number 9000-70-8 (Merck-Millipore, Darmstadt, Germany).

For *in vitro* experiments, the following materials were purchased and used without modifications: Lymphoprep (Axis-Shield, Dundee, UK); low-glucose Dulbecco's Modified Eagle Medium (D-MEM), L-glutamine, penicillin-streptomycin, trypsin, phosphate buffered saline (PBS), trypan blue, neutral red, methylene blue, P-nitrophenol, 1.5 M 2-amino-2-methyl-1-propanol, 4-nitrophenyl phosphate disodium salt hexahydrate, NaOH (all from Sigma-Aldrich); heat-inactivated fetal bovine (FBS) (Invitrogen, Carlsbad, CA, USA); PicoGreen kit (Quant-iT™; Thermo Fisher Scientific Inc., Waltham, MA, USA); tissue-culture polystyrene flasks, and ultra-low attachment (Corning, St. David's Park, UK); fluconazole (Pfizer, New York, NY, USA); absolute Et-OH (Bio-Optica, Milan, Italy); alamarBlue® (Serotec Ltd., Kidlington, UK).

Scaffold manufacturing

Hollow microfibers of PLLA and PCL were produced via dry-wet spinning, using a proprietary machine (Gimac, Castronno, Italy) located at Industrie Biomediche Insubri S/A (Mezzovico, Switzerland). This is a three-axis moving apparatus designed to co-spin, via a computer-controlled motor unit, two solutions throughout a double-annulus spinneret of submillimeter diameters, thus leading to a continuous hollow microfiber (Figure 1A).

Specifically, polymer solution and non-solvent solution, placed inside two separate syringes, converge to the spinneret passing through the outer and the inner annuli, with diameters 860 μm and 300 μm, respectively (Figure 1B). The wet fiber, as generated at its sprout, is thus collected by a Teflon rotating drum placed in air environment, designed to allow evaporation of solvents. The whole procedure is thus considered a dry-wet spinning process. Indeed, the formation of the microfiber occurs under a ternary (or multi-) phase system chemistry, which depends on the miscibility gaps of the polymer(s), solvent(s), and non-solvent(s) employed. In this study, PLLA and PCL were used as polymers, and dichloromethane as a solvent. Polymers were dissolved in dichloromethane at 1:3.5 ratio (w/v). Finally, either Et-OH or IP-OH solution containing 0.5% (w/v) G were chosen as non-solvents. The latter non-solvent solution was obtained by mixing equal volumes of IP-OH and G aqueous solution, achieved by dissolving 1% (w/v) G in double-distilled water at 50°C under stirring. After collection, the microfibers were either orderly or disorderly assembled into non-woven meshes by means of the fiber bonding technique, finally giving rise to either patterned or random fabric layouts. Briefly, predefined amounts of fibers, as produced by the dry-wet spinning process, were placed on Teflon nets and heated, under compression, to bond the microfibers together via contact points generated by controlled melting. Specifically, PLLA and PCL meshes were heated at 150°C for 1 h and 60°C for about 3 min, respectively. After bonding, the meshes were puncher-cut into discs of 15 mm diameter with about 2 mm thickness.

Microfiber and scaffold characterization

At their sprout from the spinneret, the microfibers were photographed to assess the effectiveness of manufacturing. After layout assembly, the scaffolds were mounted on aluminum stumps and sputter-coated with gold (Sputter Coater Emitech K550; Quorum Technologies Ltd., Lewes, UK) for 4 min. Scaffold and fiber morphology was observed via scanning electron microscopy (SEM) (Zeiss EVO MA10; Zeiss, Oberkochen, Germany) under an accelerating voltage of 5-10 kV. To assess maintenance of hollow morphology in the microfibers after mesh assembly, the scaffolds underwent fracture at -81°C. The microfiber diameters of the scaffold surfaces were measured on serial micrographs acquired at 100× magnification (*n*=14). Finally, the sputter-coated scaffold surfaces were photographed by means of a camera equipped for digital macro (Canon Ixus; Canon, Tokyo, Japan).

Isolation and culture of human mesenchymal stromal cells

HMSCs were isolated from bone marrow aspirates of patients admitted to our hospital for orthopedic surgery. Samples were collected after informed consent, treated anonymously and in conformity to the principles expressed

by the Declaration of Helsinki. Briefly, the bone marrow aspirate was diluted 1:4 in sterile saline and layered on Lymphoprep as a density gradient inside sterile tubes. The mononuclear cell layer, selected via centrifugation at $400 \times g$ for 25 min, was suspended in CM, containing low-glucose D-MEM, 2 mM L-glutamine, 100 U/mL penicillin, 100 mg/mL streptomycin and 10% (v%) heat-inactivated FBS. The mononuclear cells were plated at a density of $0.2 \cdot 10^5$ cells/cm² in tissue-culture polystyrene flasks. After 24 h, hMSCs were purified from other non-adherent mononuclear cells via washing with sterile saline. When the cultures reached about 80% confluence, the hMSCs were detached by using 0.25% trypsin and replated at a density of 10^3 cells/cm² to allow their expansion. Cell cultures were carried out in incubator under standard conditions, namely 37°C, 95% relative humidity, and 5% CO_2/95% air environment. An extensive characterization and multi-lineage differentiation capability of hMSCs is reported in our previous studies.[22]

Culture of human mesenchymal stromal cell/scaffold constructs

The microfiber scaffolds ($n=4$) were sterilized by overnight soaking in absolute Et-OH under ultraviolet irradiation for 1 h. After washing 10 min with a 3×antibiotics/fluconazole solution in sterile saline, the scaffolds were imbued with FBS for 30 min to favor cell adhesion. Excess FBS was removed from the scaffolds before cell seeding. HMSCs were detached with trypsin, counted under 0.2% trypan blue staining for viability evaluation, suspended in 20 μL of CM and seeded on the scaffolds at a density of 5×10^5 viable cells per scaffold. After seeding, the hMSC/scaffold constructs were placed in the incubator for 1 h to permit cell adhesion and were finally covered with CM at 5 mL/sample inside 6-well plates. Cell/scaffold constructs were cultured under standard culture conditions for 16 days, replacing CM every 3 days.

Metabolic activity of human mesenchymal stromal cell/scaffold constructs

The metabolic activity of the cells grown on the scaffolds was monitored along the culture time using the alamarBlue® assay. This bioassay incorporates a REDOX indicator resulting in color change of the CM according to cell metabolism. Moreover, it can be performed multiple times on the same samples on account of its negligible toxicity. The data were acquired according to the manufacturer's instructions and expressed as percentage of reduced alamarBlue® ($\%AB_{red}$). Briefly, samples ($n=3$) and negative controls ($n=3$), namely, media plus dye without cells, by using equa-

tion #1 from the manufacturer, were incubated for 3 h at 37°C with the alamarBlue® dye diluted in 3 mL of CM for each scaffold, according to the manufacturer's recommendations. This method for calculation against negative controls is useful to assess $\%AB_{red}$ increase of the same samples along a timeline. The total quantity of dye solution per well was chosen in theoretical excess, in order to accomplish any metabolic activity increases all the samples within 16-day cultures. Indeed, exceeding 100% of dye reduction would affect reaction kinetics, thus making any comparisons unreliable. Viability tests were performed every 3 days after seeding. At each time-point, 100 μL of supernatant from sample or control was loaded into 96-well plates; then, excess supernatant was removed from the cultures and replaced with fresh CM. The absorbance (l) of supernatants was measured with a spectrophotometer (Victor 3; PerkinElmer, Waltham, MA, USA) under a double wavelength reading (570 nm and 600 nm). Finally, $\%AB_{red}$ was calculated by correlating the absorbance values and the molar extinction coefficients of the dye at the selected wavelengths, following the protocol provided by the manufacturer. The equation applied (eq. 1) is shown below, in which, λ=absorbance, s=sample, and c=negative control:

$$\%AB_{red} = 100 \cdot \frac{(117{,}216 \cdot \lambda_{s(570\,nm)} - 80{,}586 \cdot \lambda_{s(600\,nm)})}{(155{,}677 \cdot \lambda_{c(600\,nm)} - 14{,}652 \cdot \lambda_{c(570\,nm)})}$$

Scaffold colonization by human mesenchymal stromal cells

Colonization of the scaffold surfaces by viable hMSCs was qualitatively investigated using a non-disruptive assay based on Neutral Red dye, which stains lysosomes of live cells in red. Briefly, at the endpoint, one specimen per type ($n=1$) was incubated with 50 μg/mL CM solution for 1 h. Samples were rinsed in sterile PBS and their surface was observed by means of a camera equipped for digital macro (Canon Ixus; Canon).

Methylene Blue is a stain used to visualize cells against their background, which is useful to evaluate cell adhesion and colonization on

fixed cell/polymer scaffold specimens. One MSC/scaffold construct of each type was fixed in 4% neutral buffered formalin/PBS solution at 4°C overnight. Samples were rinsed in PBS, soaked in a 0.05% Methylene Blue solution for 5 min, rinsed with double-distilled water, air-dried at room temperature. All the stained samples were observed under 3D digital microscopy (KH-7700; Hirox-USA, Hackensack, NJ, USA).

In addition, one construct per type ($n=1$) was processed for SEM analysis. Briefly it was formalin-fixed dehydrated in a graded series of ethanol aqueous solutions up to absolute Et-OH. Thereafter, dehydration of the hMSC/scaffold constructs was completed in a vacuum oven at 37°C overnight. Samples were mounted on aluminum stubs, sputter-coated with gold (Emitech K550), and observed via SEM (Zeiss EVO MA10) under an accelerating voltage of 5-10 kV. Micrographs were acquired at 302× magnifications.

Construct cellularity

At the endpoint, the double-stranded (ds) DNA (ds-DNA) content in hMSC/scaffold constructs was measured using the PicoGreen assay. On day 16, the CM was removed from each construct and replaced with 2 mL of double-distilled sterile water. Construct lysates ($n=2$) were obtained following two freeze (at -81°C for 24 h)/thawing (at 37°C for 20 min) cycles. Thawing was performed in ultrasonic bath (Falc; Progen Scientific, London, UK) set at 47 kHz frequency and 20 W output power. Standard solutions of DNA in double-distilled water at concentrations ranging in 0-6 μg/mL were prepared and 50 μL of standard or sample was loaded in a 96-well black microplate. Working buffer and PicoGreen dye solutions were prepared according to the manufacturer's instructions and added at 100 and 150 μL per well, respectively. After a 10-min incubation in the dark at room temperature, the fluorescence intensity of the samples was measured on a plate reader (Victor3; PerkinElmer), under an excitation wavelength of 485 nm and an emission wavelength of 535 nm. Ds-DNA concentration in cell lysates was thus calculated against the standard curve.

Table 1. Fiber diameters at the scaffold surfaces.

	PLLA	PCL
Patterned Et-OH	427±101	242±60
Random Et-OH	296±88	514±167
Patterned IP-OH/G	312±141	544±90
Random IP-OH/G	556±245	274±65

PLLA, poly-L-lactic acid; PCL, poly-ε-caprolactone; Et-OH, ethanol; IP-OH, isopropanol; G, gelatin. Values are reported in μm, as mean±standard deviation.

Alkaline phosphatase activity in human mesenchymal stromal cell/scaffold constructs

Intracellular ALP activity was evaluated in cascade on the same construct lysates assayed for cellularity (*n*=2) using a colorimetric end-point assay based on P-nitrophenol. Standards of P-nitrophenol were prepared in concentrations ranging from 0 to 250 μM. As necessary, the samples were diluted in double-distilled water to stay within the detection range of the assay. Therefore, individual wells of a 96-well plate were loaded as follows: 80 μL/well of standard or sample, 20 μL/well of alkaline buffer solution at pH 10.3 (1.5 M 2-amino-2-methyl-1-propanol), and 100 μL/well of 4 mg/mL ALP substrate solution (4-nitrophenyl phosphate disodium salt hexahydrate in double-distilled water). The microplate was incubated at 37°C for 1 h and 100 μL/well of 0.3 M NaOH was finally added to stop the reaction. The absorbance was then measured at 405 nm on a plate reader (Victor3; PerkinElmer). Finally, ALP activity was normalized by cellularity.

Statistical analysis

In hMSC/scaffold constructs, quantitative data were presented as mean±standard deviation. Differences were investigated by analysis of variance (ANOVA) with post-hoc *t* test. Significance was set at $P<0.05$.

Results

Scaffold fabrication and characterization

Using the dry-wet spinning apparatus shown in Figure 1, hollow microfibers based on PLLA and PCL were successfully produced using 96% vol. Et-OH or 50% vol. IP-OH/G solution as non-solvents (Figure 2A). After production, the microfibers showed hollow sections with main diameters ranging in about 250-500 μm. PLLA microfibers had a larger diameter and thinner wall (Figure 2 A1-A2) than the PCL microfibers, which showed a smaller diameter and thicker wall (Figure 2 A3-A4), independently of the non-solvent used. Upon scaffold assembly, the microfibers underwent compression and heating. Thereafter, the diameters of microfibers at the scaffold surface were imaged and measured via SEM. The morphology of scaffold layouts and microfibers is shown in Figures 2B and 3. Micrographs of PLLA are reported in Figure 3A, while those of PCL in Figure 3B. For each scaffold type, preservation of fiber cavities after compression and heating was confirmed via SEM (Figure 3, lens), although random PCL scaffolds were the most altered (Figure 3 B2, lens). Microfiber wall
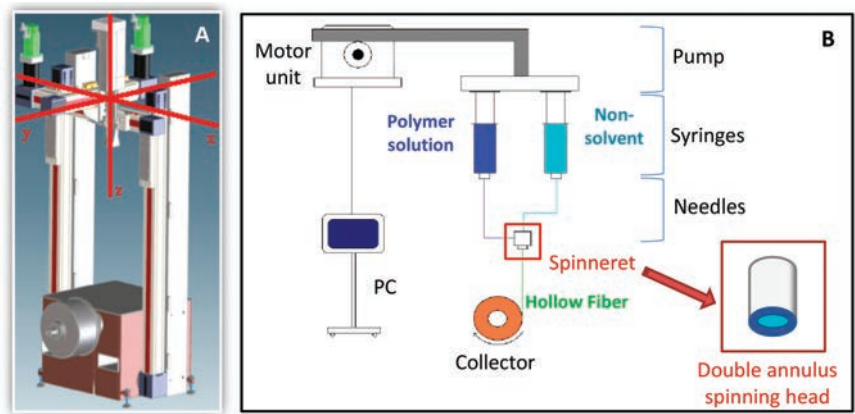
Figure 1. Scheme of the dry-wet spinning system and process: A) 3D drawing showing the spinning system and its moving axes; B) sketch representing the spinning process and key components.

thickness was measured in a one representative SEM micrograph per sample and ranged in
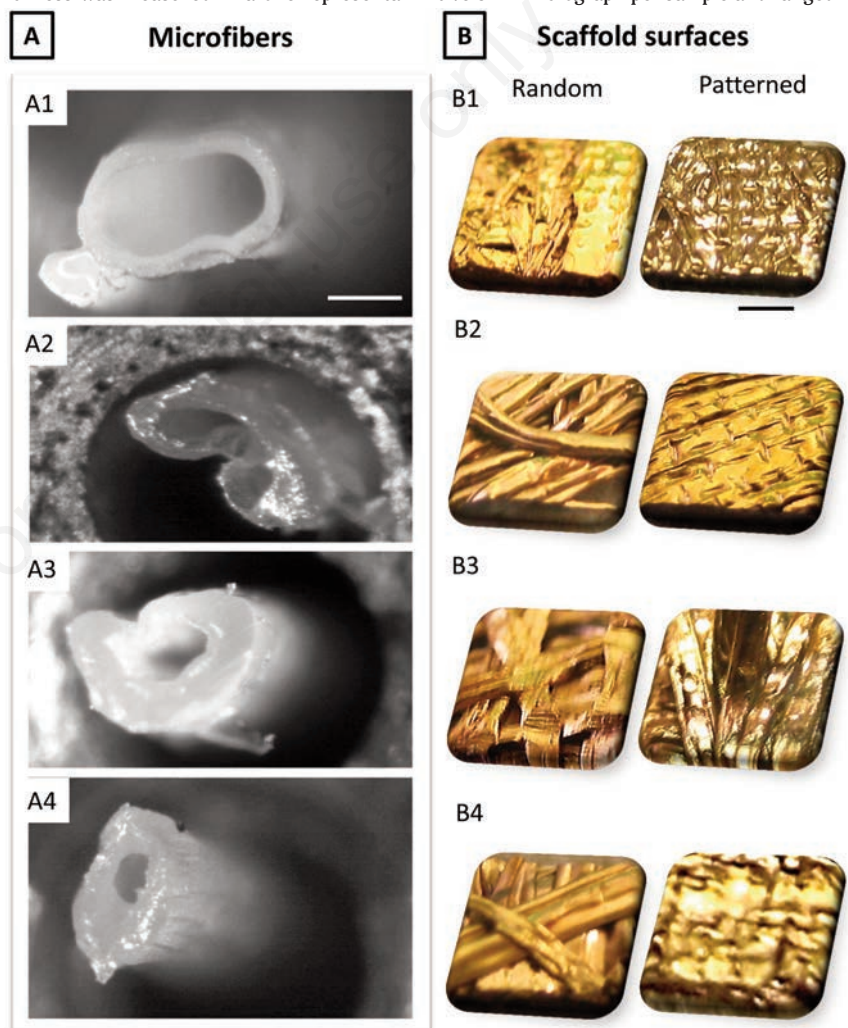
Figure 2. Photographs of hollow microfibers and scaffold surfaces. A) Hollow microfibers at their sprout from the spinneret and further identified by polymer non-solvent couples: A1) PLLA Et-OH; A2) PLLA IP-OH/G; A3) PCL Et-OH; and A4) PCL IP-OH/G. Scale bar ¼ mm. B) Photographs of scaffold surfaces sputter coated with gold, obtained via either random (left column) or ordered (right column) arrangement of microfibers: B1) PLLA Et-OH; B2) PLLA IP-OH/G; B3) PCL Et-OH; and B4) PCL IP-OH/G. Original magnification 4×, scale bar=1 mm. PLLA, poly-L-lactide; Et-OH, ethanol; IP-OH/G, iso-propanol/gelatin; PCL, poly-ε-caprolactone.

20-70 μm in PLLA, while 40-90 μm in PCL scaffolds.

At their surfaces, orderly assembled scaffolds showed tight microfiber bonding, thus resulting in lower interspaced layouts than randomly assembled fabrics. In the patterned scaffolds, the outer microfibers usually had flat morphology with evidence of intra-fiber melting and topography artefacts, such as microgrooves in PLLA and striping in PCL, probably imprinted by the Teflon nets during heating (Figures 3A and B). Differently, randomly assembled scaffolds showed best-preserved microfiber topography (Figures 3A and B). PCL microfibers were more affected by fusion and flattening induced via the fiber bonding method than PLLA ones, which, conversely, could be more easily identified and measured as single microfibers. Microfiber diameters measured at the scaffold surfaces are reported in Table 1. Owing to the artefacts generated by post-spinning processing, microfiber diameters displayed very broad sizes, ranging from 274 ± 65 μm in IP-OH/G random PCL, to 556 ± 245 μm in IP-OH/G random PLLA. No apparent trend could be observed among all the scaffolds subtypes.

## Human mesenchymal stromal cell colonization of microfiber mesh scaffolds

Using SEM analysis, adherent cells were found to be layering the microfiber surfaces at the top surface of all the scaffolds, although sometimes rarely visible because of their flat morphology and tight connections forming homogeneous cell sheets (Figure 4). Incubation with Neutral Red and staining with Methylene Blue at the endpoint allowed the viable cells colonizing the scaffolds to be easily visualized (Figures 5 and 6). Viable hMSCs were also detected on the inner microfibers of the scaffolds, which resulted to be the best colonized, as confirmed by the more intense red color. From a qualitative evaluation, cellular colonization was most pronounced in IP-OH/G random and Et-OH random PLLA (Figure 5A), and in Et-OH random PCL constructs (Figure 5B). Methylene Blue staining performed on fixed samples allowed an easier handling of the scaffolds and a better contrast against the background than those obtained in neutral red stained samples, so as to enable enhanced visualization of cells also in the inner layers (Figure 6).

Metabolic activity of human mesenchymal stromal cell/scaffold constructs

The alamarBlue® assay performed at sequential time-points up to 15 days allowed hMSC metabolism along the culture time to be monitored (Figure 7A and B). Under the applied experimental conditions of this assay, all the constructs showed initially low metabolic activity ranging from $5.28\pm0.85\%$ (in PLLA Et-OH random) to $11.80\pm0.81\%$ (in PCL Et-OH random), the latter being the highest with statistical significance among the hMSC/PCL subtypes ($P<0.05$). All the hMSC/PLLA constructs showed metabolic increases 6 days after seeding, followed by a slow decrease, which was steadily maintained until the endpoint (Figure 7A). In hMSC/PLLA constructs, the highest $AB_{red}\%$ value averagely detected was $18.03\pm3.21\%$ in the IP-OH/G random subtype on day 6, although with no statistical significance with respect to other hMSC/PLLA subtypes. On average, the PLLA IP-OH/G random constructs had a superior metabolic activity at any assayed time-point; in particular, it was the highest among the PLLA constructs from day 12 until the endpoint ($14.62\pm1.23\%$, $P<0.05$). On the other hand, all the hMSC/PCL constructs displayed picks in their metabolic activity on day 9; this was followed by a drop and a slowly decreasing trend up to the endpoint (Figure 7B). Among PCL constructs, the highest metabolic activity was found in the Et-OH random subtype, with statistical significance in the PCL series ($P<0.05$). Additionally, this value was the highest among all the constructs ($29.87\pm5.61\%$, $P<0.05$). Finally, the metabolic activity of hMSC/PCL constructs ranged from $6.75\pm0.25\%$ (Et-OH patterned) to $11.10\pm1.17\%$ (Et-OH random). The latter subtype showed an averagely superior metabolic activity at all assayed time-points.
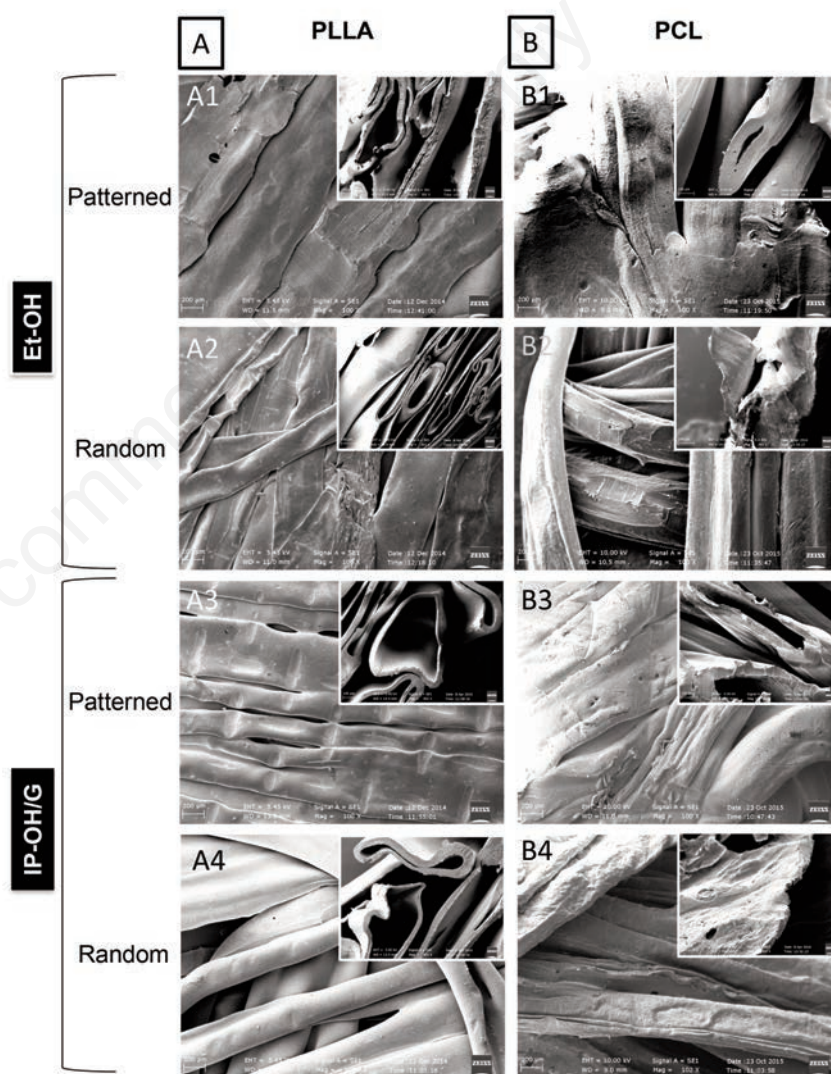
Figure 3. Scanning electron microscope (SEM) micrographs showing scaffold surfaces at the endpoint: A) poly-L-lactide (PLLA), and B) poly-ε-caprolactone (PCL). Images are grouped by non-solvent type and layout sub-type; scale bar=200 μm, 100× magnification. Lenses show SEM micrographs of hollow microfibers after scaffold fabrication; scale bar=100 μm, 302× magnification.

Human mesenchymal stromal cell function in microfiber mesh scaffolds

Intracellular ALP activity was quantified at the endpoint to assess cell function and osteo-differentiative potential on different scaffold subtypes; ALP values were normalized by cellularity (Figure 7C). ALP activity ranged from 2017 ± 324 μM/(h·μg of ds-DNA) (Et-OH patterned) to 2986 ± 295 μM/(h·μg of ds-DNA) (Et-OH random) in PLLA scaffold series, while it ranged from 1887 ± 103 μM/(h·μg of ds-DNA) (Et-OH patterned) to 3291 ± 483 μM/(h·μg of ds-DNA) (Et-OH random) in PCL scaffold series. Considering that the ds-DNA of a human diploid cell is 7.18 pg/cell, the above mentioned results mean that, at intracellular level, single hMSCs produced active ALP enzyme ranging from 0.226 ± 0.007 nM/min·cell (Et-OH patterned PCL) to 0.394 ± 0.033 nM/min cell (Et-OH random PCL), which were averagely the highest and lowest values found among all the scaffolds subtype. Unpaired t-student tests were applied to check significance between homologous subgroups differing only according to layout type. Statistical findings showed that ALP activity values of Et-OH random were significantly superior to those of Et-OH patterned subtypes, both for PLLA (P=0.00029) and PCL (P=0.0000039). No differences were similarly detected among the IP-OH/G samples. ANOVA was used to compare ALP activity under the following variables: polymer, non-solvent, and layout type. Differences in ALP activity due to the polymer type resulted to be non-significant ($F_{(1,40)}=0.30$, P=0.585). Differently, both non-solvent and layout types led to a statistically significant difference in ALP activity expression. Specifically, there were statistically significant effects of the variables non-solvent ($F_{(1,40)}=8.86$, P=0.0049) – being the values of Et-OH averagely higher than those of the IP-OH/G subgroups – and layout ($F_{(1,40)}=20.25$, P=0.000057) – since the values of random were averagely higher than those of patterned subgroups.

Discussion

Tissue engineering scaffolds have been invoked to act as cell-conditioning microenvironments.[7,8] This phenomenon has recently been disclosed as not being a prerogative of materials provided with *ad hoc* chemical modifications. In fact, the chemo-physical features of the scaffolds have been demonstrated to enable topological hints which SCs can respond with behavioral changes.[8] Therefore, the intrinsic stimulations induced by the scaf-

fold offer the intriguing possibility of addressing SC differentiation pathways, which is the subject of innovative researches.[8]

Due to the limited literature on dry-wet spun scaffolds, this investigation is very novel in the tissue-engineering scenario and can be mainly compared to other fibrous scaffold outcomes. This study was aimed at identifying some fabrication parameters in dry-wet spun microfiber scaffolding, which can affect hMSCs. In particular, polymer (PLLA *vs* PCL), non-solvent (Et-OH *vs* IP-OH/G), and fabric layout (patterned *vs* random) were tested as inherent scaffold features having possible implications for metabolic activity, 3D colonization, and function of hMSCs.

Our findings showed that the polymer influenced the metabolic activity timeline of hMSCs, while microfiber layout enhanced ALP

activity in randomly orientated scaffolds. Finally, Et-OH as a non-solvent, in combination with random microfiber assembly, showed the highest activity values for this enzyme. Therefore, the obtained results are suggestive of osteogenic lineage specification induced by randomly oriented dry-wet spun microfiber scaffolds, which could disclose possible spill-overs for bone tissue engineering applications.

The first step of this study consisted in manufacturing hollow microfibers via dry-wet spinning. The main advantages of this scaffolding technique over other fiber-based methods rely on the possibility to manufacture polymeric microfibers exploiting polymer solubility, without having to work from the molten state.[16] In this way, the chemical properties of the polymer are most preserved. There are other spinning techniques used to fabricate fibers from
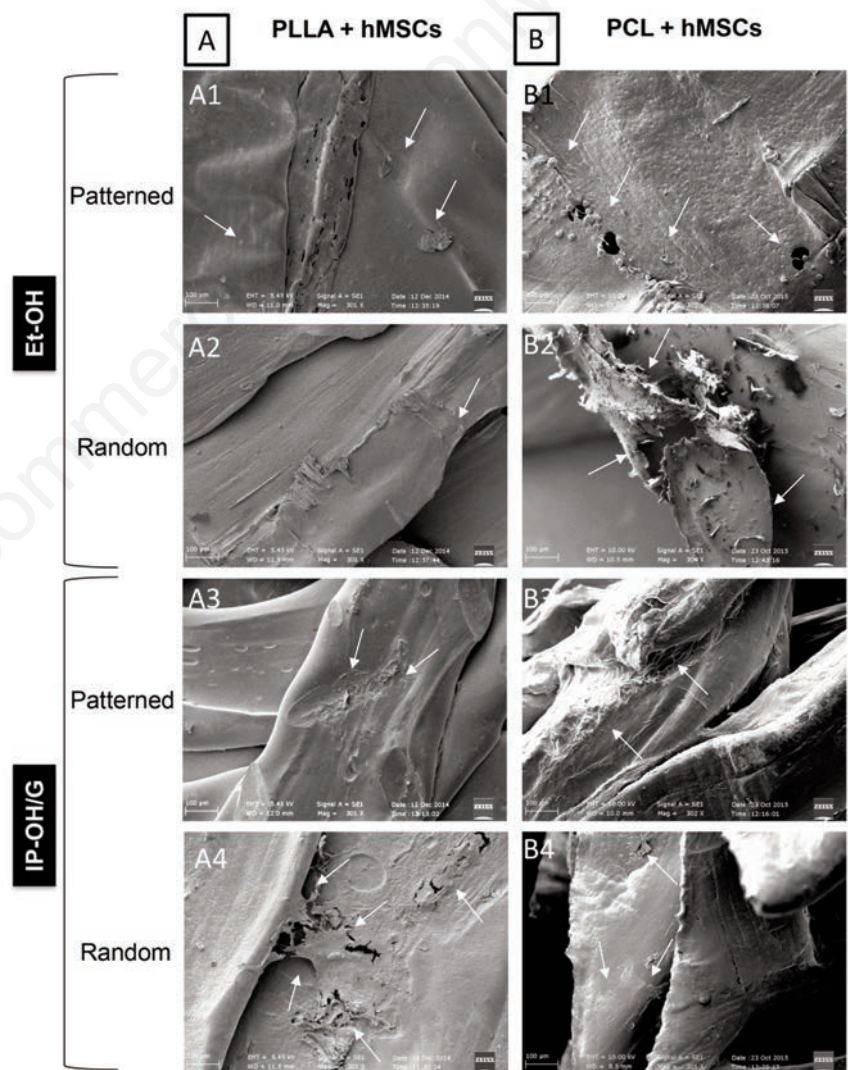
Figure 4. Scanning electron microscope micrographs showing human mesenchymal stromal cells (hMSCs) on scaffold surfaces at the endpoint: A) poly-L-lactide (PLLA), and B) poly-ε-caprolactone (PCL). Images are grouped by non-solvent type and layout sub-type. Scale bar=100 µm, 301× magnifications.

polymeric solutions, such as wet-spinning and electrospinning.[12,23,24] However, wet-spun fibers have reduced possibility for drug incorporation if compared to that of dry-wet spun fibers.[14] Finally, unlike electrospun fibers, in dry-wet spun fibers no theoretical limits exist to reach the desired thickness.[15] In this study, scaffolds with about 2 mm thickness were assembled. The methodology reported in this paper allowed the fabrication of hollow microfibers based on two bioresorbable FDA-approved polymers, namely, PLLA and PCL. Both polymers belong to the linear aliphatic polyester family, but they display some chemical differences. For example, the PCL is remarkably hydrophobic. In particular, PLLA and PCL greatly differ for their mechanical properties: PLLA is the stiffest, while PCL is the most extensible.[25]

The mechanical properties of the materials, such as rigidity, are increasingly recognized as critical regulators in MSC biology, however, their mechanism of action has only partially elucidated.[26] It has been reported that, on stiff surfaces, MSCs enhance tension and adhesiveness, which is ultimately hypothesized to modulate their lineage specification.[7]

In our experiments, the polymer type had a documented effect on the metabolic activity. Specifically, metabolism *vs* time curves of hMSCs growing on same-polymer scaffolds showed analogous trends. Metabolic raises occurred at time-points that were earlier in PLLA (day 6) than in PCL (day 9). In tissue-engineered constructs, the overall metabolic activity of cells is a useful tool to encode a number of biological information, like cytotoxicity/cytocompatibility, viability and proliferation. Of the many tests commercially available, alamarBlue® allows the metabolism of the same samples to be monitored over time with good correlation with 3D cellularity, depending on construct permeability and culture time.[27] Specifically, fibrous scaffolds offer open-pore structures which can overcome metabolite diffusion barriers in 3D constructs.[28] In our specimens, AB_{red}% averagely ranged from 5.23% on day 3 (the lowest value) to 14.62% on day 15 (the highest value). Endpoint results were qualitatively double-checked with the neutral red assay, proving the presence and density of viable cells on the meshes. Within a 2-week timeframe, the hMSC/scaffold constructs increased their metabolism at time-points that were typical for each polymer-groups, showing values up to 18.03% (PLLA, the highest value on day 6) and 29.87% (PCL, the highest value on day 9). From day 9 (PLLA) and 12 (PCL) onwards, the metabolic activity of the constructs reached a plateau, suggesting that that post-proliferative culture conditions could be reached.[27] Being the cultures carried out concomitantly, with identical test specifications and cellular batch, the trend of the metabolism

curve was attributed to a peculiar influence of the polymer type on hMSC biochemistry. Both construct colonization and metabolic activity resulted best on PLLA IP-OH/G random and PCL Et-OH random scaffold subtypes, confirming that, in our scaffolds and time-points, neither the polymer nor the non-solvent exerted a preferential role on hMSC metabolism. A dedicated study will be necessary to assess which properties (*e.g.*, chemical, physical or mechanical) of the polymers are possibly responsible for this metabolic response.
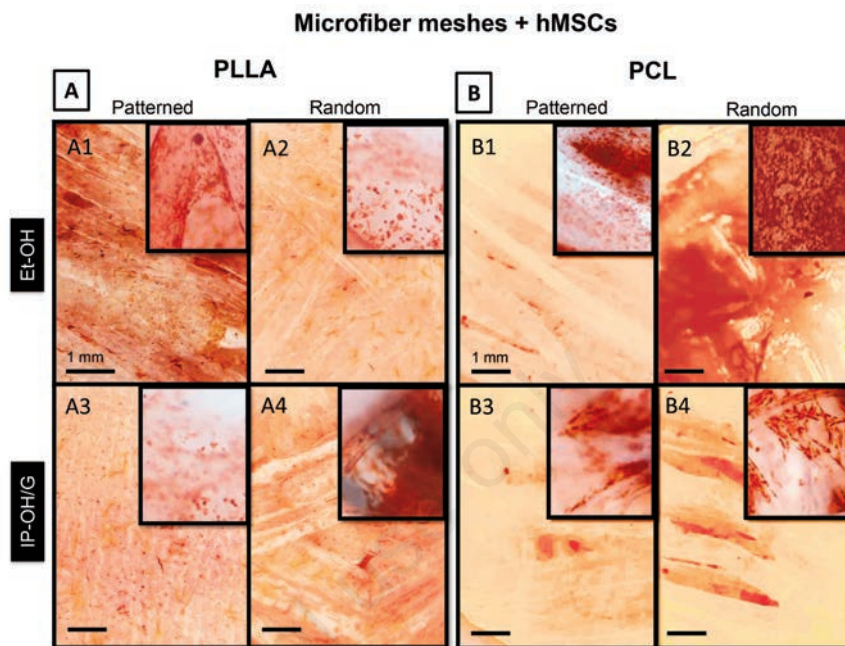
Figure 5. Photographs showing neutral red-stained human mesenchymal stromal cells (hMSCs)/scaffolds at the endpoint: A) poly-L-lactide (PLLA), and B) poly-ε-caprolactone (PCL). Main images: magnification 4×, scale bar=1 mm. Lens: digitally zoomed-in micrographs showing cell details, original magnification 35×.
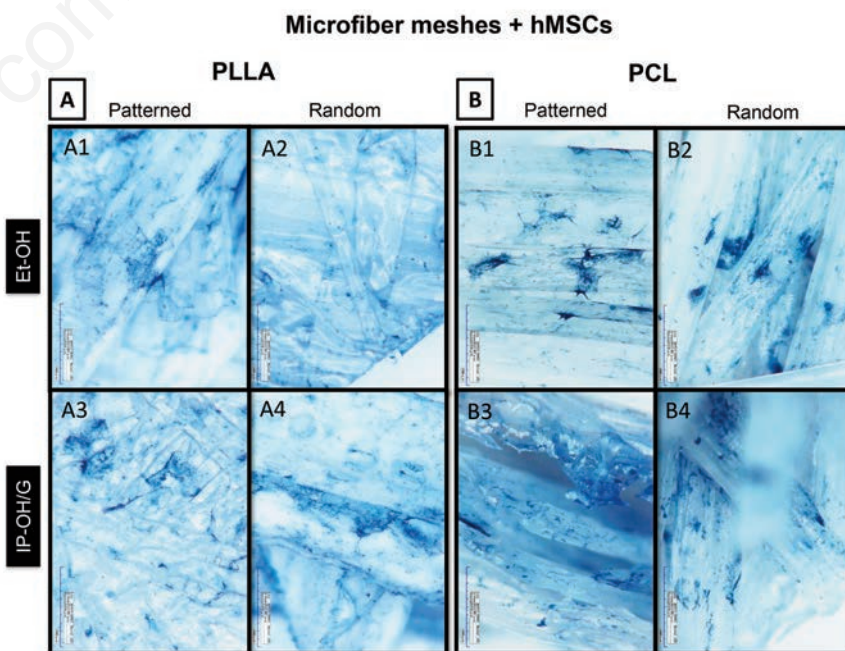
Figure 6. Stereomicroscopy images showing methylene blue-stained human mesenchymal stromal cells (hMSCs)/scaffolds at the endpoint: A) poly-L-lactide (PLLA), and B) poly-ε-caprolactone (PCL). Magnification 50×, scale bar as printed by the microscope 2000 μm.

Once the microfibers had been produced from both polymers, the fiber bonding method was applied to link them either orderly or randomly as 3D-layered structures. After spinning, fiber size ranged in 250-500 μm, showing only qualitative differences between the two polymers. These results are in line with other studies, reporting dry-wet spun PLA-(co)polymer microfibers.[14-19] The morphological analysis performed on the scaffold via SEM showed that the surface microfibers were often flattened, sometimes melted together and carrying prints from the grid used during heating, even though they maintained hollow morphology. Their average size was inhomogeneous, but it remained close to that of the fabrication range. Size differences could not be correlated to any scaffold parameters chosen for this study. The only appreciable diversity was that the random subtypes partially exposed on their surfaces second layer microfibers, which appeared morphologically preserved. Canha-Gouveia and colleagues recently showed that hierarchical features in fibrous scaffolds produced alternating orderly (3D printed) and random (electrospun) fiber layers, and had an osteogenic effect on SCs derived from Wharton's jelly.[29]

In our study, the microfiber arrangement affected the intracellular ALP activity with specificity. Many cell types are known to constitutively express ALP under different isoenzymes. However, the ALP expression in SCs has denoted particular implications, according to their hierarchical potency. For example, the ALP expression correlated very well with stemness in embryonic-like SCs, while it correlated with differentiation in adult SCs.[30] In adult hMSCs derived from the bone marrow, ALP has been recognized as a reliable marker to assess further bone forming capacity.[31] Indeed, the ALP levels induced by extrinsic cellular stimulation have shown to be predictive for the *in vivo* osteogenic differentiation capacity of these hMSCs. The study of Prins and coworkers defined the significance of this marker by assaying homogeneous subpopulations of bone marrow hMSCs, selected from one heterogeneous population.[31] In our experiments, the same hMSC batch was equally divided into all the different scaffold types, each type broken up into multiple numbers. No differentiative supplements were added in the CM, so that any significant difference in ALP activity expression is likely to be the result of a physical conditioning of the scaffold as a microenvironment. The detected differences between ALP activity expressed by hMSCs in patterned and random scaffolds showed remarkable statistical significance under the ANOVA test ($P=0.000057$), indicating potential for osteogenic lineage specification driven by random layout geometry. According to published papers, the obtained ALP values are comparable to those of trabecular bone fragments or
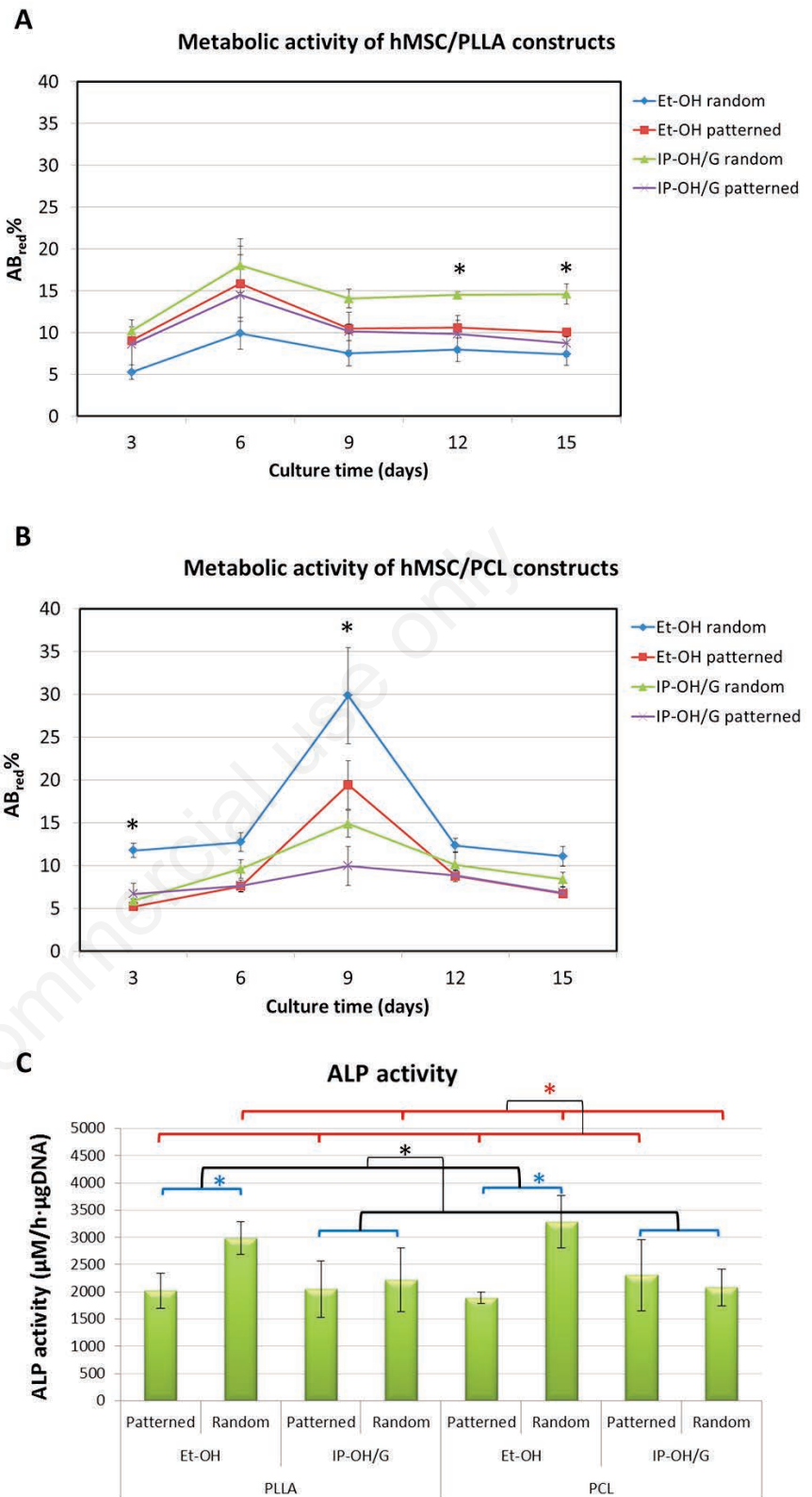

Figure 7. Bar graphs showing the results of quantitative tests: A-B) metabolic activity over culture time of human mesenchymal stromal cells (hMSCs) grown in poly-L-lactide (PLLA) and poly-ε-caprolactone (PCL) scaffolds; and C) expression of intracellular alkaline phosphatase (ALP) activity per cell at the endpoint. *$P<0.05$.

bone marrow cultured *in vitro* with osteogenic supplements for 15 days, while they are higher than those usually detected in MSCs or bone cells grown on culture plastics.[32] It is worth noting that the expression of ALP, like other markers, results to be frequently increased in 3D-culture systems.

Finally, some specific influence of the non-solvent was detected upon ALP activity expression. The microfibers spun by using Et-OH as a non-solvent showed, on average, significantly highly values (P=0.0049) of ALP activity versus those produced with IP-OH/G. This statistical difference was less notable than that calculated by comparing random versus patterned layouts. The combination of random and Et-OH thus showed the highest ALP activity values. In this study, two volatile non-solvents, Et-OH and IP-OH, were used at concentrations that were chosen to balancing their potential toxicity.[33] The microfibers were dried upon collection, and post-processed in oven, which allowed solvent and non-solvent evaporation. The absence of cytotoxic effects, as from metabolic and viability assays discussed earlier, corroborated the effective removal of any toxic components from the scaffolds and are in line with observations conducted with dry-wet spun PLLA (co)polymers.[14-19] From a technological standpoint, the polymer/solvent/non-solvent thermodynamic system determines the miscibility gaps and the equilibrium phases controlling the morphological features of the fiber.[14,16] Under the applied conditions, phase separation did not cause fiber nanoporosity. In their study on spongy scaffolds, Viswanathan and colleagues highlighted that SC adhesion was dependent on topology and chemistry, and independent of porosity. They also showed that topology, architecture and interconnectivity affected the SC osteogenic differentiation potential.[8] At this early stage of our investigation it is not possible to hypothesize any valuable reasons explaining the role played by the non-solvent in these fibrous scaffolds. Only further studies could ascertain hMSC/random microfiber scaffold bone formation capacity *in vitro* and *in vivo* and whether the non-solvent makes a true difference. It can be hypothesized that other physical characteristics of the materials, such as surface roughness and hydrophilicity, may affect hMSC behavior.

Tuning scaffold features intelligently to address SC fate will enable the development of smart scaffolds that could catalyze the desired tissue formation from immature cells, helping to discourage SC trans-differentiation and tissue overgrowth, which are the actual concerns of translational therapies.

Conclusions

In this study we investigated the influence of polymer, non-solvent and scaffold layout of dry-wet microfiber scaffolds on metabolic activity, colonization and ALP activity expression of bone marrow hMSCs. The polymer type affected the timeline trend of metabolic activity. Both construct colonization and metabolic activity resulted to be independent of other scaffold subtypes. Instead, hMSCs grown on random microfiber fabrics averagely showed statistically superior intracellular ALP activity per cell to that detected on patterned fabrics. The highest ALP values were detected in the Et-OH random subtypes. Although the underlying mechanisms of cell-substrate interaction leading to ALP increase and metabolic behavior still need to be elucidated, the outcomes reported in this study propose new insights into fibrous scaffolds like SC conditioning microenvironments, which could concur to pave the way for future strategic directions in SC tissue engineering.

References

1. Langer R, Vacanti JP. Tissue engineering. Science 1993;260:920-6.
2. Lysaght MJ, Reyes J. The growth of tissue engineering. Tissue Eng 2001;7:485-93.
3. Cosson S, Otte EA, Hezaveh H, Cooper-White JJ. Concise review: tailoring bioengineered scaffolds for stem cell applications in tissue engineering and regenerative medicine. Stem Cells Transl Med 2015;4:156-64.
4. Wei CC, Lin AB, Hung SC. Mesenchymal stem cells in regenerative medicine for musculoskeletal diseases: bench, bedside, and industry. Cell Transplant 2014;23:505-12.
5. Tatullo M, Marrelli M, Paduano F. The regenerative medicine in oral and maxillofacial surgery: the most important innovations in the clinical application of mesenchymal stem cells. Int J Med Sci 2015;12:72-7.
6. Yeatts AB, Choquette DT, Fisher JP. Bioreactors to influence stem cell fate: augmentation of mesenchymal stem cell signaling pathways via dynamic culture systems. Biochim Biophys Acta 2013;1830:2470-80.
7. Huang C, Dai J, Zhang XA. Environmental physical cues determine the lineage specification of mesenchymal stem cells. Biochim Biophys Acta 2015;1850:1261-6.
8. Viswanathan P, Ondeck MG, Chirasatitsin S, et al. 3D surface topology guides stem cell adhesion and differentiation. Biomaterials 2015;52:40-7.
9. Borenstein JT, Weinberg EJ, Orrick BK, et al. Microfabrication of three-dimensional engineered scaffolds. Tissue Eng 2007;13:1837-44.
10. Tamayol A, Akbari M, Annabi N, et al. Fiber-based tissue engineering: progress, challenges, and opportunities. Biotechnol Adv 2014;31:669-87.
11. Piskin E, Bölgen N, Egri S, Isoglu IA. Electrospun matrices made of poly(alpha-hydroxy acids) for medical use. Nanomedicine 2007;2:441-57.
12. Kumbar SG, James R, Nukavarapu SP, Laurencin CT. Electrospun nanofiber scaffolds: engineering soft tissues. Biomed Mater 2008;3:034002.
13. Danti S, Mota C, D'Alessandro D, et al. Tissue engineering of the tympanic membrane using electrospun PEOT/PBT copolymer scaffolds: a morphological in vitro study. Hearing Balance Commun 2015;13:133-47.
14. Lazzeri L, Cascone MG, Quiriconi S, et al. Biodegradable hollow microfibres to produce bioactive scaffolds. Polym Int 2005;54:101-7.
15. Ellis MJ, Chaudhuri JB. Poly(lactic-co-glycolic acid) hollow fibre membranes for use as a tissue engineering scaffold. Biotechnol Bioeng 2007;96:177-87.
16. Pertici G, Maccagnan S, Müller M, et al. Porous biodegradable microtubes-based scaffolds for tissue engineering, part I: production and preliminary in vitro evaluation. J Appl Biomat Biomech 2008;6:186-92.
17. Danti S, Ciofani G, Pertici G, et al. Boron nitride nanotube-functionalised myoblast/microfibre constructs: a nanotech-assisted tissue-engineered platform for muscle stimulation. J Tissue Eng Regen Med 2015;9:847-51.
18. Barachini S, Trombi L, Danti S, et al. Morpho-functional characterization of human mesenchymal stem cells from umbilical cord blood for potential uses in regenerative medicine. Stem Cells Dev 2009;18:293-305.
19. D'Alessandro D, Pertici G, Moscato S, et al. Processing large-diameter poly(L-lactic acid) microfiber mesh/mesenchymal stromal cell constructs via resin embedding: an efficient histologic method. Biomed Mater 2014;9:045007.
20. Holzwarth JM, Ma PX. Biomimetic nanofibrous scaffolds for bone tissue engineering. Biomaterials 2011;32:9622-9.
21. Mota C, Danti S, D'Alessandro D, et al. Multiscale fabrication of biomimetic scaf-

folds for tympanic membrane tissue engineering. Biofabrication 2015;7:025005.

22. Trombi L, Mattii L, Pacini S, et al. Human autologous plasma-derived clot as a biological scaffold for mesenchymal stem cells in treatment of orthopedic healing. J Orthop Res 2008;26:176-83.

23. Mariani M, Rosatini F, Vozzi G, et al. Characterization of tissue-engineered scaffolds microfabricated with PAM. Tissue Eng 2006;12:547-57.

24. Puppi D, Mota C, Gazzarri M, et al. Additive manufacturing of wet-spun polymeric scaffolds for bone tissue engineering. Biomed Microdev 2012;14:1115-27.

25. Middleton JC, Tipton AJ. Synthetic biodegradable polymers as orthopedic devices. Biomaterials 2000;21:2335-46.

26. Hao J, Zhang Y, Jing D, et al. Mechanobiology of mesenchymal stem cells: perspective into mechanical induction of MSC fate. Acta Biomaterialia 2015;20:1-9.

27. Zhou X, Holsbeeks I, Impens S, et al. Noninvasive real-time monitoring by alamarBlue(®) during in vitro culture of three-dimensional tissue-engineered bone constructs. Tissue Eng 2013;19:720-9.

28. Wilson CE, Dhert WJ, Van Blitterswijk CA, et al. Evaluating 3D bone tissue engineered constructs with different seeding densities using the alamarBlue assay and the effect on in vivo bone formation. J Mater Sci-Mater M 2002;13:1265-9.

29. Canha-Gouveia A, Rita Costa-Pinto A, Martins AM, et al. Hierarchical scaffolds enhance osteogenic differentiation of human Wharton's jelly derived stem cells. Biofabrication 2015;7:035009.

30. Štefková K, Procházková J, Pacherník J. Alkaline phosphatase in stem cells. Stem Cells Int 2015;2015:1-11.

31. Prins HJ, Braat AK, Gawlitta D, et al. In vitro induction of alkaline phosphatase levels predicts in vivo bone forming capacity of human bone marrow stromal cells. Stem Cell Res 2014;12:428-40.

32. Hoemann CD, El-Gabalawy H, McKee MD. In vitro osteogenesis assays: influence of the primary cell source on alkaline phosphatase activity and mineralization. Pathol Biol 2009;57:318-23.

33. Gossel TA. Alcohols, glycols and aldehydes. In: Gossel TA, JD Bricker, eds. Principles of clinical toxicology. 3rd ed. London: Taylor & Francis; 2001. pp.75-98.